Ships and Offshore Structures

ISSN: 1744-5302 (Print) 1754-212X (Online) Journal homepage: www.tandfonline.com/journals/tsos20

Quantifying operational variability across ship types and size classes in the North and Baltic Seas

Joost Hobbie, Ishan Sontakke, Thorben Schwedt, Martin Bergström & Sören Ehlers

To cite this article: Joost Hobbie, Ishan Sontakke, Thorben Schwedt, Martin Bergström & Sören Ehlers (17 Apr 2026): Quantifying operational variability across ship types and size classes in the North and Baltic Seas, Ships and Offshore Structures, DOI: 10.1080/17445302.2026.2656938

To link to this article: https://doi.org/10.1080/17445302.2026.2656938

Published online: 17 Apr 2026.

SHIPS AND OFFSHORE STRUCTURES
https://doi.org/10.1080/17445302.2026.2656938

Quantifying operational variability across ship types and size classes in the North and Baltic Seas

Joost Hobbie, Ishan Sontakke, Thorben Schwedt, Martin Bergström and Sören Ehlers

German Aerospace Center (DLR e.V.), Institute of Maritime Technologies and Propulsion Systems, Geesthacht, Germany

ABSTRACT

This study quantifies operational variability across major ship types and size classes in the North and Baltic Seas using one year of AIS data. A framework of twelve operational metrics is developed to capture key dimensions of ship operations and aggregated into variability scores at ship-type and size-class level. Results reveal clear structural differences: cargo segments such as container, vehicle, and bulk carriers exhibit low variability and highly standardized operations, while passenger and service vessels show pronounced heterogeneity. Variability generally decreases with vessel size, indicating increasing operational standardization. Decomposition analysis identifies engine performance and energy use as primary drivers of variability, followed by routing and loading, while speed plays a minor role. Sensitivity analyses confirm robustness across weighting schemes. The findings provide empirically grounded reference values for improving fleet-level emission and compliance models and support more realistic assessments of maritime decarbonization strategies.

ARTICLE HISTORY
Received 30 October 2025
Accepted 26 January 2026

KEYWORDS
Ship; operations; decarbonization; North Sea; Baltic Sea; AIS

1. Introduction

1.1. Background

Well-informed policy- and decision-making in the context of maritime decarbonization requires accurate modeling of ship operations. Shipping carries about 80% of global trade by volume (UNCTAD 2021) and remains indispensable for global connectivity (Rodrigue 2024), yet accounts for roughly 3% of anthropogenic CO_2 emissions. Achieving the revised IMO target of net-zero emissions by or around 2050 (IMO 2023) – together with regional measures such as the EU ETS extension (EU 2024) and FuelEU Maritime (EU 2023) – requires a realistic, data-driven understanding of how ships actually operate rather than how they are designed to perform.

Operational patterns determine the timing, magnitude, and distribution of energy use and emissions across routes and fleet segments. Modeling these patterns accurately is therefore crucial for linking technical characteristics – such as installed power or design speed – to real-world performance and regulatory outcomes. However, many fleet- and policy-level models assume uniform operational behavior, which can distort projections of fuel demand and emissions-reduction potential.

The increasing availability of AIS data enables detailed reconstruction of vessel movements and operational profiles, offering insight into real-world fleet activity. Building on this empirical foundation, the present study contributes to a more realistic representation of ship operations in decarbonization research by analyzing how operational patterns vary across ship types and size classes.

Nomenclature

AE:	Auxiliary Engine
AIS:	Automatic Identification System
CBM:	Cubic Meter
CII:	Carbon Intensity Indicator
CO_2:	Carbon Dioxide
DNV:	Det Norske Veritas
DWT:	Deadweight Tonnage
EMSA:	European Maritime Safety Agency
ETS:	Emission Trading System
EU:	European Union
GHG:	Greenhouse Gas
GT:	Gross Tonnage
IALA:	International Association of Marine Aids to Navigation and Lighthouse Authorities
IHO:	International Hydrographic Organization
IMO:	International Maritime Organization
KN:	Knots
KWh:	Kilowatt Hour
LNG:	Liquefied Natural Gas

CONTACT Joost Hobbie joost.hobbie@dlr.de DLR Institute of Maritime Technologies and Propulsion Systems, Düneberger Straße 108, Geesthacht 21502, Germany

ME: Main Engine
MMSI: Maritime Mobile Service Identity
MoSES: Modular Ship Emission Modeling System
NM: Nautical Mile
Ro-Pax: Roll-on/Roll-off Passenger
Ro-Ro: Roll-on/Roll-off
SEIM: Shipping Emission Inventory Model
SOG: Speed Over Ground
SOLAS: International Convention for the Safety of Life at Sea
STEAM: Ship Traffic Emission Assessment Model
TEU: Twenty-foot Equivalent Unit
UNCLOS: United Nations Convention on the Law of the Sea
UNCTAD: United Nations Conference on Trade and Development

1.2. Related work

Accurate representation of ship operations is fundamental for estimating fuel consumption and emissions (Kim and Choi 2023), and for evaluating the feasibility and impact of low-carbon technologies (Elmallah et al. 2025). Research in maritime emissions and fleet modeling has evolved from aggregated bottom-up approaches toward data-driven analyses of real operations and, more recently, toward integrating these empirical insights into techno-economic and decarbonization frameworks. This progression underscores the growing recognition that operational diversity must be captured to improve the accuracy of fleet-level assessments.

Early bottom-up frameworks combined vessel characteristics, engineering models, and emission factors to estimate fuel use at global or regional scales. The Fourth IMO GHG Study (IMO 2021) established a methodological foundation by merging AIS data with ship technical information and predefined operational modes, refining earlier emission inventory approaches (IMO 2015). Tools such as STEAM (Jalkanen et al. 2016), the approach of Olmer et al. (2017), MoSES (Schwarzkopf et al. 2021), and SEIM (Yi et al. 2025) reconstruct ship trajectories and embed resistance and engine models to estimate emissions at high spatial and temporal resolution. Similar methodologies have been applied in the North Sea and adjacent waters (Aulinger et al. 2016). While indispensable for emission inventories and scenario analyses, these frameworks offer limited visibility into the dispersion of ship operations within and across fleet segments.

To address this limitation, research has increasingly focused on empirical analyses of ship operations. Trivyza et al. (2016) showed that even small shifts in speed distributions can substantially affect energy use and lifecycle emissions. Jafarzadeh and Schjølberg (2018) analyzed AIS data from Norwegian waters for eight ship types and found large variations in load profiles – particularly for offshore and passenger vessels – identifying them as promising candidates for hybrid or electric propulsion. Zhou et al. (2019) advanced ship operations analysis by applying clustering methods to AIS data from the Port of Rotterdam, demonstrating that multidimensional vessel descriptors improve classification accuracy. Complementary deep-learning approaches, such as the neural-network-based classifier by Chen et al. (2020) further improved motion-state detection, while Martincic et al. (2020) proposed validation techniques to reduce misclassification among operational phases. Collectively, these studies expanded the methodological toolbox for deriving high-fidelity operational states from large AIS datasets.

Building on these foundations, later work linked operational data directly to specific use cases. Oh et al. (2021) combined AIS and oceanographic data to analyze container-vessel operations, revealing company-specific behaviors, substantial speed variability, and frequent port-waiting periods. Park and Choi (2022) used k-means clustering to derive representative speed-time profiles for electric patrol vessels, showing that real operations often deviate from design expectations, leading to oversizing of propulsion systems. Fan et al. (2024) constructed typical operating conditions from millions of data points, reproducing energy use and emissions more accurately than standardized test cycles. Similarly, Godet et al. (2024) developed standardized operational cycles for container ships, inspired by automotive drive cycles, which reduced the inherent variability of CII indicators and provided consistent efficiency benchmarks.

These empirical insights have recently been incorporated into techno-economic and decarbonization models. Comer et al. (2022) linked AIS-derived trading patterns with energy modeling to assess hydrogen and wind-assisted propulsion for bulk carriers in the North and Baltic Seas, underscoring the need for realistic operational data in technology assessment. Bergström et al. (2023) employed discrete-event simulation to evaluate compliance with EEXI and CII regulations for ships calling at German ports, showing that vessel-specific operating profiles are critical for predicting retrofit needs and speed-reduction strategies. Kanchiralla et al. (2023) combined life-cycle assessment and costing for different ship types, demonstrating that the technical and economic feasibility of alternative fuels depends strongly on operational patterns.

1.3. Research scope

Despite substantial progress in data-driven ship operations research, quantitative assessments of operational

variability across ship types and size classes remain scarce. Most studies focus on individual vessel categories or case studies, limiting cross-fleet comparability. Consequently, the representativeness of key operational parameters – such as operating mode-specific time allocation, speed, and engine load – remains uncertain. This is critical because these parameters constitute core inputs to bottom-up ship energy and emission models, directly determining propulsion power demand, fuel consumption, and associated emissions. Generalized assumptions regarding these parameters at fleet level therefore may obscure operational diversity within and across fleet segments and introduce uncertainty into model outputs of energy and fuel use, emissions, as well as technology performance and regulatory compliance.

In particular, misrepresenting speed distributions, ME loads, or the share of time spent in specific operational modes can lead to systematically biased energy and emission estimates. Such biases may further distort techno-economic evaluations on emission mitigation measures and affect conclusions on the suitability of alternative fuels or energy-saving devices, thereby ultimately influencing strategic decision-making on newbuild and retrofit activity, alternative fuel infrastructure planning, and legislation. This reemphasizes the widely acknowledged need for realistic, empirically grounded operational contexts as a prerequisite for robust techno-economic assessments of maritime decarbonization strategies at fleet level (DNV 2025a).

Against this background, the present study quantifies and compares the operational variability of major ship types and size classes operating in the North and Baltic Seas, using one year of AIS data. The North Sea and the Baltic Sea differ in specific physical and trade characteristics; however, both are generally characterized by dense traffic, a broad spectrum of ship types, a high frequency of port calls, and stringent regulatory frameworks (ABL Group 2021), thereby providing data-rich and well-defined conditions for the systematic analysis of ship operations. Their joint analysis therefore offers a consistent empirical basis for assessing operational variability across ship types and sizes.

While absolute operational characteristics – such as average speed levels, routing patterns, or port-related behavior – may vary across geographic regions, the focus of this study lies on relative variability and representativeness within ship type and size segments. These patterns are primarily driven by vessel design, operational role, and service profile rather than by geography alone. Accordingly, the methodological framework is not region-specific and can be applied to other sea areas, although absolute reference values may differ.

The study investigates (i) whether distinct operational patterns can be identified among ship types, (ii) which operational dimensions drive variability within and across fleet segments, and (iii) how diversity across size classes affects the representativeness of generalized assumptions commonly applied in fleet-level models. By translating the observed operational dispersion into comparable variability metrics, the study provides a solid empirical basis for distinguishing between fleet segments with highly standardized behavior and those characterized by pronounced heterogeneity. For ship types exhibiting low operational variability, representative parameter values – such as average speed, ME load, or phase-specific time shares – can be meaningfully applied in fleet-level modeling. In contrast, segments with high operational dispersion require modeling approaches that either retain vessel-specific parameterization or explicitly account for uncertainty and variability in operational inputs. The resulting reference values therefore support more realistic fleet representations in energy and emissions modeling approaches and enable more robust assessments of decarbonization and mitigation strategies.

The remainder of this paper is structured as follows: Section 2 describes the methodological framework; Section 3 presents and interprets the results, including ship-type and size-bin variability; Section 4 discusses the implications, limitations, and future research avenues; and Section 5 summarizes the key findings of the paper.

2. Materials and methods

2.1. Methodological framework

This study systematically derives, classifies, and evaluates ship operational characteristics from high-resolution AIS data. Figure 1 summarizes the sequential workflow. The subsections below describe each methodological step in detail.

2.2. AIS data and fleet initialization

The analysis draws on AIS observations of vessels operating in the North and Baltic Seas, two of the most intensely trafficked and regulated maritime regions worldwide, including designated emission control areas and comprehensive AIS monitoring systems (HELCOM 2009). The dense AIS receiver coverage and high frequency of regularly operating vessels in these regions support robust reconstruction of vessel trajectories and operational states.

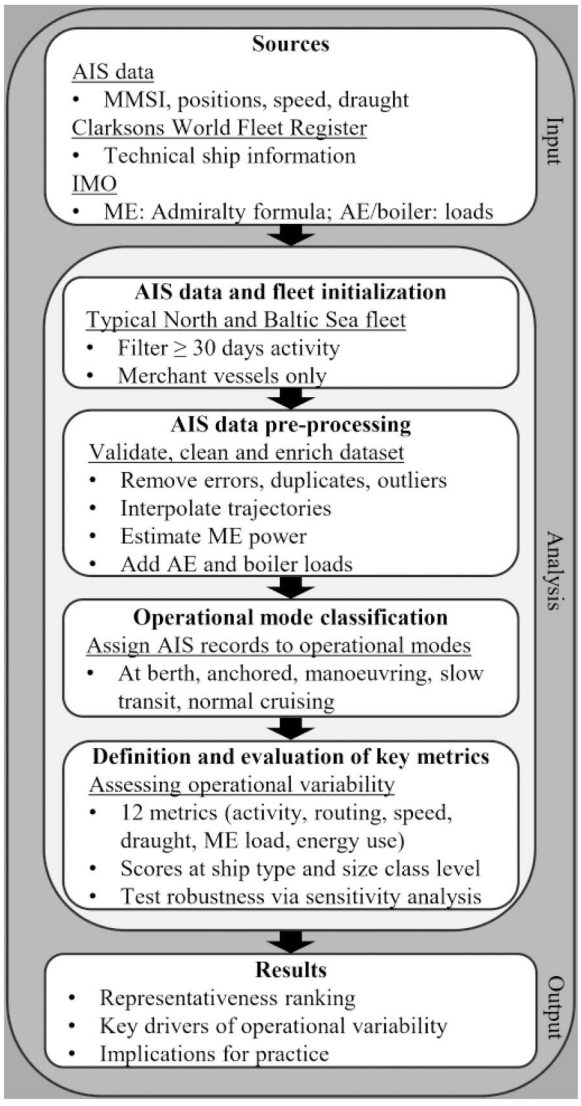

Figure 1. Methodological framework for assessing operational variability across ship types and size classes using AIS data.

AIS is a standardized vessel-tracking system that continuously transmits dynamic parameters (e.g. position, speed, draught) alongside static identifiers (e.g. MMSI, call sign, principal dimensions) (IALA 2016). These transmissions enable high-resolution reconstruction of vessel trajectories and provide a robust empirical basis for analyzing operational behavior.

The dataset covers 2019 to reflect representative pre-pandemic operations and to avoid related distortions in trade and fleet deployment (EMSA 2021). To focus on vessels with sustained regional activity, ships were required to transmit AIS within the study area for at least 30 days. This criterion excludes transient traffic and retains vessels with regular operations. The geographical extent of the North and Baltic Seas follows IHO (1953) definitions and is implemented using shapefiles from the Flanders Marine Institute (2018). From this subset, only merchant vessels were included; non-commercial ships (e.g. fishing, private leisure) typically exhibit irregular, purpose-specific activity not representative of commercial operations (Kontopoulos et al. 2021).

AIS identifiers were matched to technical records from Clarksons Research (2025) to obtain ship-specific technical properties and enable classification by type and size. Specifically, vessels were first matched from the AIS dataset to the Clarksons database by mapping MMSI numbers. Based on a match, each vessel was assigned a ship-specific classification using the corresponding Clarksons 'Fleet Type' and 'Type' entries, rather than relying on AIS-reported ship type codes.

As this study follows the IMO (2021) categorization, the Clarksons-based ship types were subsequently mapped to IMO ship type categories through a harmonization step, ensuring consistency with the taxonomy used in the Fourth IMO GHG Study (2021). In most cases, vessels were assigned to IMO type bins directly via the Clarksons Fleet Type field (e.g. Clarksons Fleet Type: Containerships → IMO Ship type: Container); for heterogeneous categories – Ferry-RoPax, Ferry-pax only, and service vessels – additional subtype information ensured consistent mapping (e.g. Clarksons Fleet Type: Pass./Car Catamaran Vessel, Pass./Car Ferry, Passenger/Cargo Vessel, Ro-Ro Freight/Passenger → IMO Ship type: Ro-Pax ferry).

After filtering and matching, the dataset comprised 5,241 ships, assigned to 16 ship types and 67 type-size combinations. Vessel size bins are defined using ship-type-specific capacity measures, following the size-class definitions applied in the Fourth IMO GHG Study (IMO 2021). Depending on the ship type, vessel size is classified by DWT (bulk carrier, chemical tanker, refrigerated bulk, general cargo, oil tanker, other liquids tanker, Ro-Ro), GT (cruise, ferry-RoPax, ferry-pax only, vehicle, offshore, service – other, service – tugs) container capacity TEU (container), or volume in CBM (liquefied gas tanker). Lower size bins correspond to smaller vessels and higher bins to progressively larger vessels within each ship type; absolute bin boundaries therefore differ across ship types and are not directly comparable. Table 1 summarizes the analyzed fleet.

To ensure statistical robustness, only categories with at least ten vessels were retained for subsequent analysis. This filtering yielded a final dataset of 5,188 merchant ships across 14 ship types and 49 type-size combinations. This cohort provides a representative cross-section of commercial activity in the North and Baltic Seas and forms the empirical foundation for assessing operational variability.

Table 1. Composition of the analyzed fleet by ship type and size bin.

Ship type	Size bin 1	2	3	4	5	6	7	8	9	Total
Bulk carrier	0	113	137	194	18	1	–	–	–	463
Chemical tanker	77	131	138	25	6	–	–	–	–	377
Container	92	63	28	63	36	44	20	37	29	412
Cruise	2	6	21	23	15	2	–	–	–	69
Ferry-pax only	148	68	4	3	-	-	-	-	-	223
Ferry-RoPax	178	44	18	24	63	-	-	-	-	327
General cargo	696	290	116	34	-	-	-	-	-	1,136
Liquefied gas tanker	5	0	1	0	-	-	-	-	-	6
Offshore	518	-	-	-	-	-	-	-	-	518
Oil tanker	81	28	2	170	13	126	27	7	-	454
Other liquids tanker	3	4	-	-	-	-	-	-	-	7
Refrigerated bulk	2	16	5	30	-	-	-	-	-	53
Ro-Ro	12	24	42	29	-	-	-	-	-	107
Service – other	428	-	-	-	-	-	-	-	-	428
Service – tugs	613	-	-	-	-	-	-	-	-	613
Vehicle	17	12	19	-	-	-	-	-	-	48

Note: Size-bin boundaries follow the ship-type specific capacity classes defined in the IMO GHG Study 2021 (IMO 2021). For brevity, the numerical ranges are not reproduced here.

2.3. AIS data pre-processing

Despite their high spatial and temporal resolution, AIS records exhibit coverage gaps, accuracy issues, and completeness challenges due to transmission losses, interference, and manual input errors (Harati-Mokhtari et al. 2007). Systematic pre-processing is therefore required before conducting quantitative analysis (Zhao et al. 2018).

Following the Fourth IMO GHG Study (IMO 2021) pre-processing comprised three stages: (i) error correction and filtering, (ii) gap filling, and (iii) estimation of ME power demand and total energy use, which are described in the following sections.

In the first step, messages with invalid positions (latitude $< -90°$ or $> 90°$; longitude $< -180°$ or $> 180°$) were removed, and duplicates arising from multiple transponders or repeated transmissions were eliminated. In addition, recorded SOG values exceeding 20 KN were capped at 20 KN. That is, reported speeds above this threshold were limited to 20 KN, while the corresponding AIS records were otherwise retained unchanged. The rationale for this approach is twofold. First, propulsion power scales non-linearly with speed, such that a small number of extreme values can disproportionately affect the related aggregated engine and energy metrics presented in Table 3. Second, within the adopted operational mode classification described in Section 2.4, all speeds above five KN are treated equivalently. As a result, the applied speed cap does not affect metrics that are related to operational mode assignment. However, potential limiting implications of this treatment for high-speed segments, such as ferries, are discussed separately in Section 4.2 Limitations.

In the second step, continuous vessel trajectories were reconstructed via linear interpolation along great-circle arcs at 90-second intervals, resulting in uniformly sampled trajectories. This reconstruction introduces additional trajectory points between recorded AIS messages, for which no original SOG or draught information is available. For such reconstructed points, SOG values were imputed based on neighboring observations: when bounded by valid AIS messages, missing SOG values were assigned the mean of the preceding and subsequent recorded speeds. In cases where multiple consecutive interpolated points occurred between two recorded AIS messages, the same linear interpolation principle was applied consistently across the gap. This approach ensures continuity of the speed profile without introducing artificial acceleration or deceleration across short data gaps. AIS draught information was treated consistently with this aggregation-based approach. Rather than being handled as a high-frequency time-varying signal, draught was treated as a voyage-level parameter. Vessel trajectories were segmented into voyages, defined as the time interval between the end of one port stay and the beginning of the next, where a port stay was identified as a continuous period of at least one hour within port proximity. For each voyage, a single representative draught value was derived as the median of all AIS-reported draught values within that voyage and assigned uniformly to all corresponding AIS records. No pointwise smoothing or jump filtering was applied to the raw draught time series; robustness was achieved through voyage-level aggregation and the use of the median, which strongly reduces the influence of isolated erroneous or poorly refreshed AIS messages. This treatment is consistent with the operational assumption that loading and unloading predominantly occur in port and that draught remains approximately constant over the duration of a voyage aside from gradual changes due to fuel and ballast consumption or water density variations (Derrett 2005).

Overall, approximately 11% of all records in the final dataset correspond to reconstructed trajectory points, while the remaining observations originate directly from recorded AIS messages. Figure 2 shows the resulting spatial density of AIS observations across the study area, highlighting the main maritime corridors represented in the dataset.

After pre-processing, vessel-specific energy demand was derived from the processed AIS dataset. Consistent with IMO (2021), instantaneous ME power demand ($\dot{W}_i$) was estimated using an adapted Admiralty formulation as per Equation (1):

$$\dot{W}_i = \frac{\delta_w \cdot W_{ref} \cdot \left(\frac{t_i}{t_{ref}}\right)^m \cdot \left(\frac{v_i}{v_{ref}}\right)^n}{\eta_w \cdot \eta_f} \quad (1)$$

where W_{ref}, t_{ref}, and v_{ref} are the vessel's reference ME power, draught, and speed from Clarksons Research (2025); v_i (SOG) and t_i (draught) are derived from AIS. Exponents $m = 0.66$ and $n = 3$ capture empirical relationships between draught, speed, and power demand. A uniform fouling correction factor $\eta_f = 0.917$ represents a ~9% resistance increase; the weather factor η_w varied by ship type and size (0.909 for smaller vessels, ~10% increase; 0.867 for larger vessels, ~15% increase). A speed-power correction δ_w accounted for service-speed deviations: $\delta_w = 0.75$ for large container ships (> 14,500 TEU), $\delta_w = 0.70$ for cruise vessels, and $\delta_w = 1$ for all others. The resulting instantaneous ME load was then obtained by normalizing the estimated ME power demand against the vessel's installed ME power obtained from Clarksons Research (2025), yielding a dimensionless utilization factor between zero and one, with exceeding values capped at one.

To complement propulsion power, AE and boiler loads were added to obtain total energy demand. AE and boiler power values were adopted from IMO (2021) by ship type, size class, and operational mode. Four modes were distinguished, consistent with Section 2.4: at berth, anchored, maneuvering, and at sea (including slow transit and normal cruising). For each mode, fixed AE and boiler power levels were assigned by vessel category.

Total instantaneous power for each AIS record was then:

$$\dot{P}_i^{tot} = \dot{W}_i + P_{AE,mode} + P_{B,mode} \quad (2)$$

Instantaneous values ($\dot{W}_i$ and $\dot{P}_i^{tot}$) were multiplied by the AIS-based 90-second-interval and integrated over time to derive cumulative ME and total energy demand, respectively.

2.4. Operational mode classification

To enable structured, comparable analysis, the pre-processed AIS dataset was classified into standardized operational modes. Ship behavior varies by location and context – from stationary port operations to low-speed maneuvering and open-sea passages (Li et al. 2024). A clear distinction among activity modes is therefore essential.

Mode assignment followed a rule-based framework combining three AIS-derived indicators: SOG, ME load, and distance to the nearest port and coastline.

While SOG and ME load were obtained directly from the processed AIS dataset, distances to port and coastline were derived from Natural Earth geospatial datasets at 10 m resolution (Natural Earth 2009a, 2009b), using

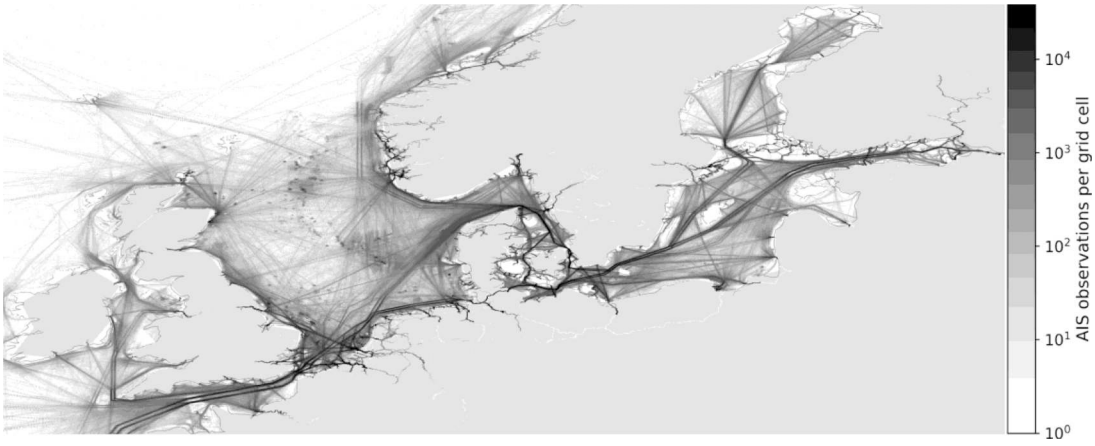

Figure 2. Spatial density of AIS observations in the North and Baltic Seas of the analyzed dataset. The map shows the aggregated number of AIS position reports per grid cell. Darker shades indicate higher densities; the color scale is logarithmically normalized to enhance visibility of both major shipping corridors and low-traffic areas.

nearest-neighbor queries. For each AIS position, port distance was defined as the distance to the nearest port point, and coast distance as the minimum great-circle distance to the nearest coastline point. To reduce sensitivity to small-scale shoreline features and ensure computational efficiency, coastline geometries were moderately simplified prior to processing using a tolerance of 0.01°. Distances were applied consistently across the study area and interpreted only in combination with SOG and ME load within the rule set.

Based on these parameters, each AIS record was assigned to one of five modes: at berth, anchored, maneuvering, slow transit, or normal cruising. Threshold combinations are summarized in Table 2.

This procedure links each AIS observation to a defined operational state, transforming raw trajectories into a structured operations dataset. The mode labels provide a consistent foundation for subsequent analyses, including time allocation, speed, and ME load by mode.

2.5. Definition and evaluation of key metrics

To quantify variability across ship types and sizes, twelve key metrics were defined. These indicators span the principal dimensions of ship behavior and enable a multi-dimensional assessment of operating patterns.

Table 3 summarizes the metrics, grouped into six categories, along with weighting factors that are varied later in sensitivity analyses.

- **Activity.** Annual distance sailed is the cumulative great-circle distance between consecutive AIS positions; the share of time in sailing modes (normal cruising, slow transit, maneuvering) indicates the fraction of time under propulsion relative to total operational time.
- **Routing.** A 500 NM threshold distinguishes long-distance voyages from short-sea operations. This aligns with short-range connectivity in Tsiotas and Ducruet (2021), corresponds to DNV (2022) regional operations in Northern Europe, and remains below the SOLAS (IMO 1914) short-international-voyage limit (< 600 NM). The share of sailing time occurring more than 12 NM from the nearest port or coastline differentiates open-sea from coastal navigation, following the territorial-water boundary defined by UNCLOS (UN 1984).
- **Speed.** The time-weighted mean SOG across sailing modes represents typical cruising speed; the corresponding standard deviation captures propulsion steadiness.
- **Draught.** The time-weighted mean draught represents typical loading; its standard deviation captures fluctuations in cargo utilization.
- **Engine.** The time-weighted mean ME load denotes average utilization of installed propulsion power during sailing; ME load deviation quantifies variations in power demand. Both rely on instantaneous estimates from Equation (1).
- **Energy.** Total energy use integrates ME, AE, and boiler power per Equation (2). Energy use per NM (sailing modes) normalizes by annual sailing distance and serves as a propulsion-efficiency indicator.

For each ship type and size bin, the standard deviation of each metric (σ_i) was computed across vessels to quantify intra-group dispersion. The twelve indicators were then aggregated into a single variability score per type–size combination via a weighted mean of standard deviations as per Equation (3):

$$\sigma_{\text{size}} = \frac{\sum_{i=1}^{12} w_i \cdot \sigma_i}{\sum_{i=1}^{12} w_i} \tag{3}$$

where σ_i is the metric-specific standard deviation and w_i the assigned weight. In the baseline, all metrics were equally weighted ($w_i = 1$). A sensitivity analysis assessed robustness to alternative weighting schemes.

Ship-type variability was then computed as the average across size bins according to Equation (4):

$$\sigma_{\text{type}} = \frac{1}{n} \sum_{j=1}^{n} \sigma_{\text{size},j} \tag{4}$$

Table 2. Operational mode assignment matrix (IMO 2021).

SOG (KN)	ME load	Port distance (NM)		Coast distance (NM)		
		≤ 1	1–5	≤ 1	1–5	≥ 5
1 ≤	–	At berth	At berth*	Anchored	Anchored	Anchored
1–3	–	Anchored	Anchored*	Anchored	Anchored	Anchored
3–5	≤ 0.65	Maneuvering	Maneuvering*	Maneuvering	Maneuvering	Slow transit
	> 0.65	Maneuvering	Maneuvering*	Maneuvering	Maneuvering	Normal cruising
> 5	≤ 0.65	Maneuvering	Slow transit*	Slow transit	Slow transit	Slow transit
	> 0.65	Maneuvering	Normal cruising*	Normal cruising	Normal cruising	Normal cruising

* Applicable to chemical tankers, liquified gas tankers, oil tankers and other liquids tankers only.

Table 3. Overview of operational metrics and weighting scheme.

Category	Metrics	Weight
Activity	Distance sailed; share of time in sailing mode	1–2
Routing	Share of long voyages; time ≥ 12 NM from coast	1–2
Speed	Average speed; speed deviation	1–2
Draught	Average draught; draught deviation	1–2
Engine	Average ME load; ME load deviation	1–2
Energy	Total energy use; energy use per NM	1–2

where n is the number of size bins within a ship type and j indexes bins.

To test robustness against unequal sample sizes across bins, an alternative weighted formulation was applied in Equation (5):

$$\sigma_{\text{type, weighted}} = \frac{\sum_{b=1}^{n} N_b \sigma_{size,b}}{\sum_{b=1}^{n} N_b} \quad (5)$$

with N_b denoting the number of vessels in bin b and n is the number of bins per ship type. This weighting assigns proportionally greater influence to bins with larger fleet representation.

Lower values of σ_{size} and σ_{type} indicate uniform operational profiles; higher values indicate heterogeneous activity. For interpretability, representativeness thresholds were defined as:

- High representativeness class: $\sigma_{type/size} < 25\%$
- Medium representativeness class: $25\% \leq \sigma_{type/size} < 50\%$
- Low representativeness class: $\sigma_{type/size} \geq 50\%$

3. Results

3.1. Operational variability across ship types

Substantial contrasts emerge in how consistently different ship types operate within the North and Baltic Seas. The aggregated variability index (σ_{type}) quantifies the internal consistency of operational behavior within each ship type, averaged across all size bins. Table 4 summarizes the variability levels and corresponding representativeness ranks and classes.

Cargo-dominated segments – particularly liner services such as container and vehicle carriers, but also bulk carriers – exhibit comparatively low operational variability, reflecting highly standardized service schedules and well-established trading routes that result in consistent and predictable operating patterns (Ksciuk et al. 2023). Refrigerated bulk, chemical tankers, cruise, general cargo, oil tankers, and Ro-Ro vessels display moderate variability, reflecting a broader but still comparable range of operating patterns and a balance between scheduled and mission-specific deployment. In contrast, passenger- and service-oriented vessels exhibit markedly higher dispersion, reflecting the operational flexibility required to meet fluctuating transport demand, diverse service missions, and regionally differing route networks.

To identify which aspects of vessel behavior drive these differences, the aggregated variability index (σ_{type}) was decomposed into the six operational metric categories, representing distinct functional dimensions of ship operations as defined in Section 2.5. For each ship type, the twelve underlying metrics were first grouped into these categories, and their mean relative deviations were normalized by the total variability of that ship type. Figure 3 therefore presents a normalized decomposition of operational variability within each ship type. Each bar represents a breakdown of the total observed variability, showing how strongly different operational dimensions – such as routing, speed, or ME load – contribute to that variability. The percentages do not reflect the number of ships, the frequency of observations, or traffic intensity. By construction, each row in Figure 3 sums to 100% and should be interpreted exclusively as a within-type attribution of variability drivers, rather than as a population- or frequency-weighted comparison across ship types. The figure thus highlights which operational domains dominate variability for a given ship type, providing structural insight into the sources of heterogeneity rather than differences in fleet size or data volume.

The decomposition highlights pronounced contrasts across fleet segments. Activity-related metrics contribute moderately overall but reach up to 27.9% for general cargo ships, reflecting substantial differences in sailing-time shares and annual distances traveled within this class, and thus indicating heterogeneous deployment

Table 4. Operational variability at the ship type level (σ_{type}) for vessels operating in the North and Baltic Seas.

Ship type	σ_{type} [%]	Rank	Representativeness	Ship type	σ_{type} [%]	Rank	Representativeness
Container	22.1	1	High	Oil tanker	40.3	8	Medium
Vehicle	22.5	2	High	Ro-Ro	41.3	9	Medium
Bulk carrier	22.6	3	High	Ferry-RoPax	96.4	10	Low
Refrigerated bulk	25.2	4	Medium	Service – tugs	120.6	11	Low
Chemical tanker	29.1	5	Medium	Service – other	130.3	12	Low
Cruise	30.3	6	Medium	Offshore	144.3	13	Low
General cargo	36.6	7	Medium	Ferry-pax only	152.6	14	Low

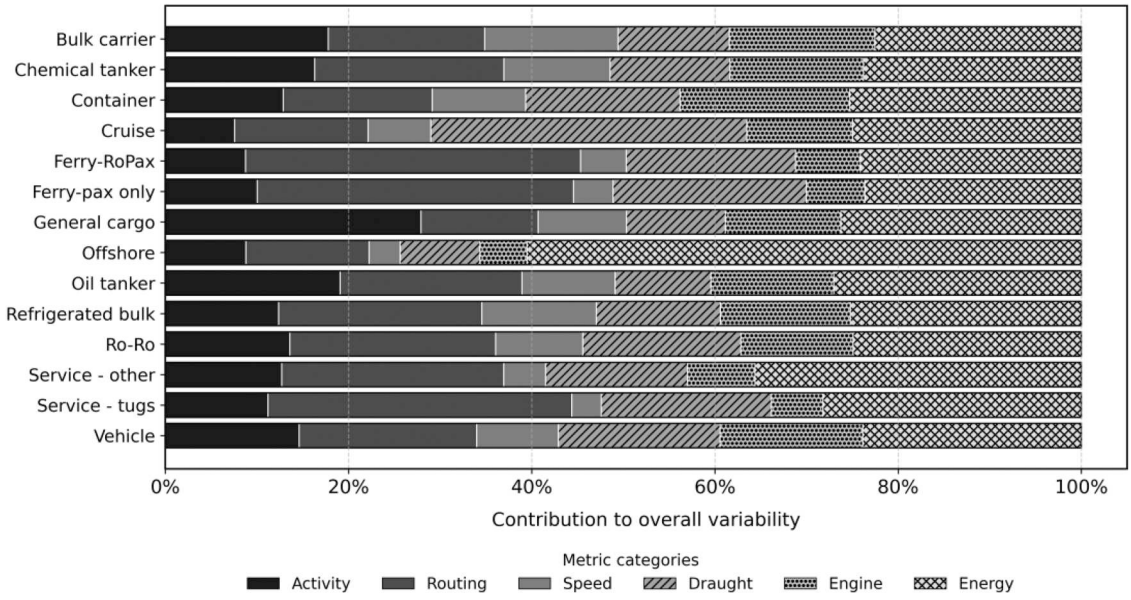

Figure 3. Normalized decomposition of the aggregated operational variability index (σ_{type}) by ship type. Each bar represents a 100% breakdown of the total operational variability within a ship type, showing the relative contribution of the six operational metric categories. Percentages indicate contributions to variability.

intensity and service regularity. Routing-related variability dominates for passenger and service categories – Ferry-RoPax (36.6%), Ferry-pax only (34.5%), and Service – tugs (33.2%) – reflecting the diversity of operational areas and route characteristics, ranging from short coastal connections to longer open-sea passages. Speed-related variability contributes less overall (3-15%) and peaks for bulk carriers (14.5%), suggesting largely standardized sailing speeds across most ship types, consistent with fuel-efficiency targets and cost-optimization strategies pursued by ship operators (Ramboll 2022). Draught-related variability is particularly high for cruise vessels (34.5%), and remains notable for vehicle (17.6%) and container ships (16.9%), reflecting not only fluctuating loading conditions and passenger volumes, but – especially for cruise vessels – pronounced differences in vessel design and deployment, ranging from small coastal cruise ships with frequent port calls and associated draught adjustments to large ocean-going cruise liners operating on multi-day sea passages with comparatively stable draught levels. Engine load variability (5-18%) is highest for container (18.5%), bulk (15.9%), and chemical tankers (14.6%), indicating differing propulsion utilization even within otherwise standardized trades. Finally, energy-related metrics explain the largest share of total variability in most categories (typically 23-27%) and peak at 60.5% for offshore vessels, underlining that propulsion demand and energy intensity are key drivers of intra-type variation.

To evaluate the robustness of the aggregated variability indicator (σ_{type}) against unequal sample sizes across size bins, two formulations were compared: (i) the baseline case, in which σ_{type} was calculated as the unweighted mean of all size-bin variability scores as per Equation (4), and (ii) a weighted variant accounting for the number of vessels in each size bin as per Table 1 and Equation (5). Table 5 compares the resulting weighted variability values with the baseline results and reports the relative deviations (Δ_{rel}) and rank changes in representativeness.

The weighting analysis confirms that σ_{type} remains largely stable across ship types, showing only moderate sensitivity to unequal sample sizes. Most deviations are below 10%, indicating that the aggregated indicator is

Table 5. Sensitivity of ship-type variability (σ_{type}) to vessel-count weighting across size bins.

Ship type	$\sigma_{type,\ weighted}$ [%]	Δ_{rel} [%]	Rank	Ship type	$\sigma_{type,\ weighted}$ [%]	Δ_{rel} [%]	Rank
Container	23.8	7.8	1 → 3	Oil tanker	37.8	−6.2	8
Vehicle	23.2	3.4	2	Ro-Ro	34.5	−16.4	9 → 7
Bulk carrier	24.1	6.7	3 → 4	Ferry-RoPax	134.3	39.4	10 → 12
Refrigerated bulk	23.0	−8.6	4 → 1	Service – tugs	-	-	11 → 10
Chemical tanker	29.0	−0.3	5	Service – other			12 → 11
Cruise	30.2	−0.4	6	Offshore	-	-	13
General cargo	42.7	16.6	7 → 9	Ferry-pax only	159.3	4.4	14

robust against fleet-size imbalances. Larger deviations for general cargo, Ro-Ro, and Ferry-RoPax reflect uneven size-bin distributions and the particularly heterogeneous behavior of vessels within small size bins, which are overrepresented in these categories. Only one change in representativeness occurs – refrigerated bulk carriers now fall into the high representativeness category – while other differences affect rank order rather than interpretation.

3.2. Operational variability across ship types and size classes

While the previous section addressed variability at the ship-type level, this part explores how operational consistency varies across size bins. Vessel size influences behavior through differences in cargo capacity, route accessibility, and fuel efficiency (Stopford 2009). To capture these effects, the variability index σ_{size} was calculated for each size bin within every ship type, providing a more granular view of intra-type dispersion.

Figures 4–6 illustrate these results by representativeness class. Each plot shows σ_{size} by size bin, with horizontal reference lines at 25% and 50% marking the thresholds between high, medium, and low representativeness. Ship types with only one size bin (offshore, service – other, service – tugs) were excluded from this analysis.

Container ships, vehicle carriers, and bulk carriers exhibit uniformly low variability, remaining near or below the 25% threshold across most size classes. Variability generally decreases with vessel size – except for vehicle carriers in size bin 3 – indicating that larger ships operate under more standardized and predictable service conditions. For container ships in particular, this trend reflects the increasing operational specialization and network integration associated with vessel upsizing: larger units are typically deployed on fixed, long-haul routes with regular schedules and stable cargo demand, whereas smaller vessels serve regional or feeder trades characterized by more flexible routing and variable port sequences (Cullinane and Khanna 2000). Consequently, size-dependent variability within these segments mirrors the hierarchical structure of global liner networks, where operational regularity rises with vessel size and market concentration.

Refrigerated bulk, chemical tankers, cruise ships, general cargo, oil tankers, and Ro-Ro vessels show broader, partly size-dependent variability (25%–50%). The smallest units (size bin 1 – and size bin 2 for general cargo) exhibit the highest variability, especially among oil tankers and Ro-Ro vessels. Consistent with the patterns observed above, this indicates that smaller units operate in more flexible and less uniform patterns – likely due to their involvement in variable service missions, shorter coastal routes, or ad-hoc charters – whereas larger vessels display increasingly homogeneous operational behavior, anchored in stable trades or defined service contracts (Sys et al. 2008).

Ferry-RoPax and Ferry-pax only vessels exhibit extreme variability across all size bins, far exceeding the 50% threshold. Even the largest ferries remain inconsistent, reflecting demand-driven, schedule-sensitive operations with limited structural regularity. As noted by Gucma and Raczkowska (2018), even large

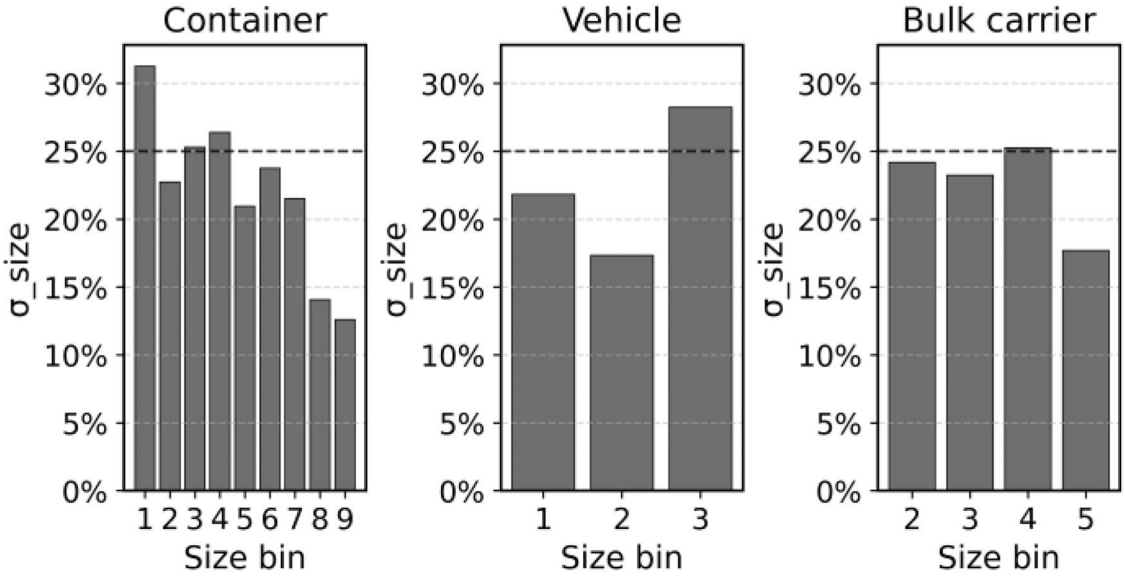

Figure 4. Size-bin-specific operational variability (σ_{size}) for high-representativeness ship types.

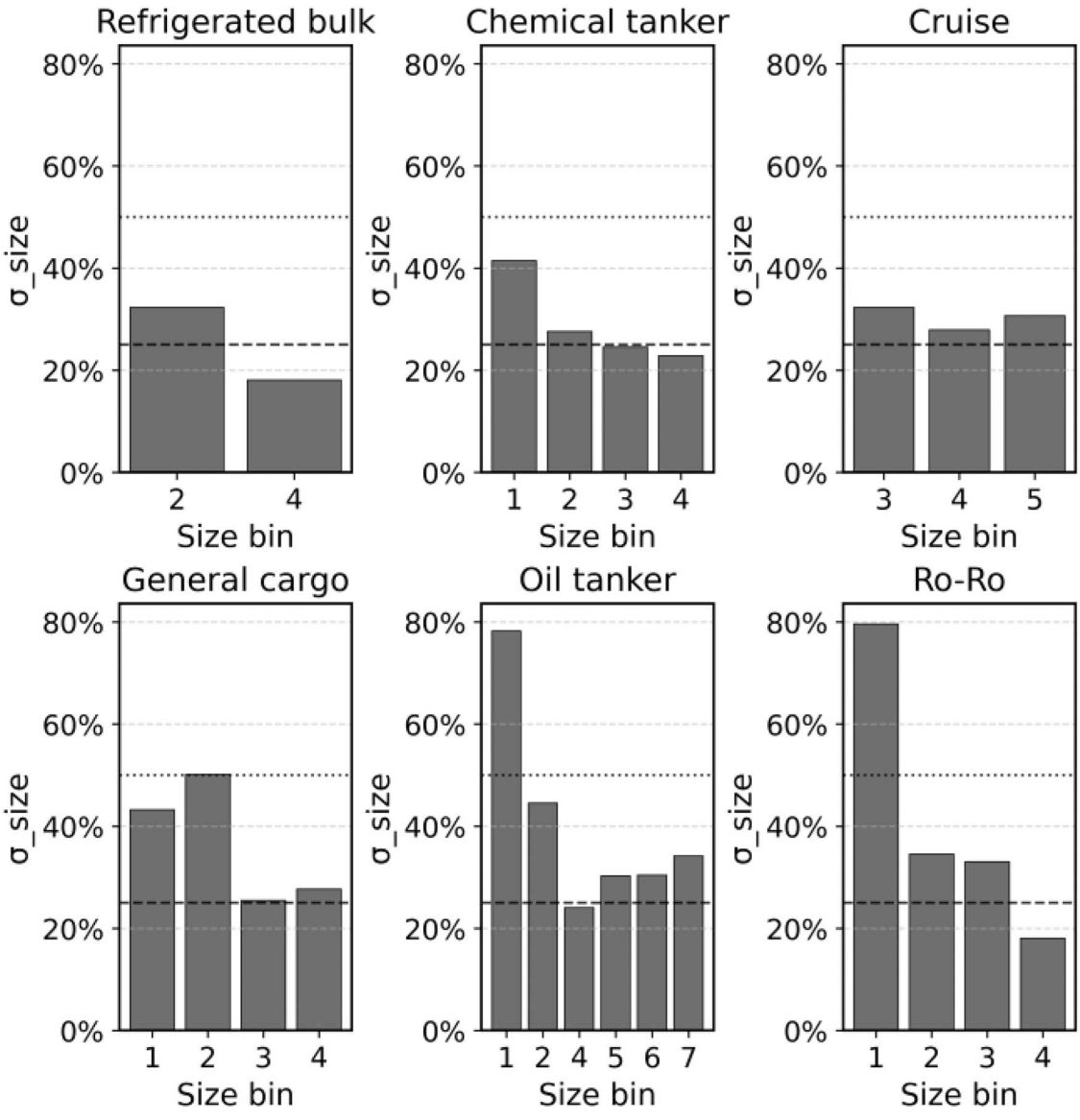

Figure 5. Size-bin-specific operational variability (σ_{size}) for medium-representativeness ship types.

Ro-Pax ferries show considerable variation in design and service characteristics – such as capacity, power, and route profiles – leading to equally diverse operational behaviors that contrast sharply with the standardized configurations and operating patterns of large cargo vessels. Frequent departures, seasonal fluctuations in passenger and vehicle demand, and the geographic constraints of fixed port networks further contribute to irregular service patterns and highly dynamic utilization levels. Consequently, their operational variability reflects the intrinsic flexibility required to balance service continuity with fluctuating transport demand.

In summary, vessel size exerts a stabilizing influence in structured liner cargo segments but has little effect for passenger and service ships. Larger industrial carriers – particularly container, bulk, and vehicle ships – operate along standardized, route-bound routines, whereas smaller or passenger-oriented vessels maintain flexible and heterogeneous patterns. These findings indicate that size-based segmentation is suitable for industrial cargo types, while functional segmentation may provide a more accurate representation of variability in dynamic and demand-driven fleets.

To evaluate the influence of metric weighting on size-bin variability (σ_{size}), three schemes were compared: (i) an equal-weight baseline (as shown above), (ii) a differentiated scheme assigning higher weights ($w_i = 2$) to fundamental descriptors of vessel operation – time in sailing and open-sea phases, average speed, engine load, draught, and energy use per NM, and (iii) a random-weighting scenario with w_i randomly distributed between 1 and 2.

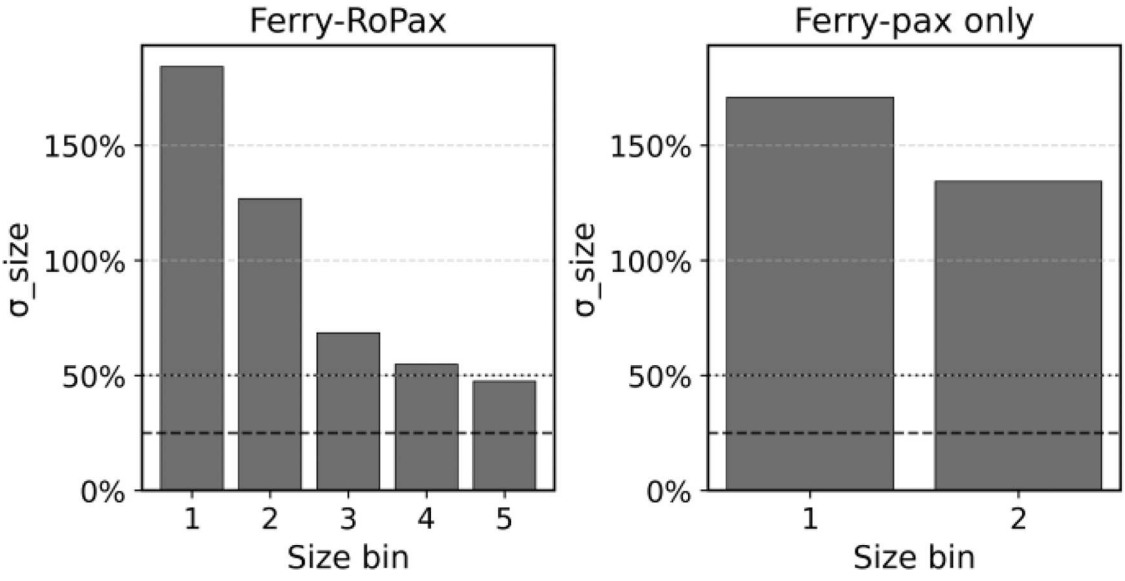

Figure 6. Size-bin-specific operational variability (σ_{size}) for low-representativeness ship types.

Across all ship types, σ_{size} remain highly consistent across weighting schemes, with average deviations of 4.7% and no change in the representativeness classification. The maximum deviation (27.7%) occurs for offshore vessels, while passenger and service categories (e.g. Ferry-RoPax, service – other) show moderate differences (5-10%). For all major cargo segments, deviations remain below 3%, confirming that the observed decline of σ_{size} with vessel size is structurally robust and not an artefact of metric weighting.

4. Discussion

4.1. Implications

By quantifying the dispersion of key operational parameters within ship types and size classes, this study moves beyond the assumption that average ship operational profiles are universally representative. Instead, it provides a data-driven basis to distinguish between segments where mean values constitute robust modeling inputs and segments where averaging obscures substantial operational heterogeneity. In this way, observed operational variability is translated directly into guidance on when simplified modeling assumptions are defensible and when they are not.

This distinction becomes evident when comparing major ship types and purposes. Operational variability in the North and Baltic Seas is strongly structured by ship function and, to a lesser extent, by vessel size. This structure directly constrains fleet-level energy and emissions modeling, as it determines the extent to which simplified operational assumptions can be applied without distorting energy demand, emissions, compliance outcomes, or technology feasibility studies. Cargo segments that operate on fixed networks (notably container, vehicle, and bulk carriers) display comparatively uniform behavior, which legitimizes the use of standardized duty cycles and stable parameter sets. In contrast, passenger and service segments exhibit high dispersion in operational profiles, indicating that single-profile representations are insufficient and that operational heterogeneity must be represented explicitly.

Three implications for modeling practice follow directly. First, the quantified variability indicators provide a practical criterion for deciding when average operational profiles are sufficient and when uncertainty must be represented explicitly. For ship types with low operational variability, central tendency measures – such as mean speed, mean ME load, or average energy demand per NM – constitute robust and defensible parameter values. In contrast, segments characterized by high operational variability require uncertainty-aware parameterization, for example through wider parameter ranges or explicit dispersion measures, in order to avoid systematic misrepresentation of operational behavior.

Second, the choice of fleet segmentation should reflect the stability of operational behavior within the fleet segment. For liner cargo, type-level segmentation often suffices and can be refined with size segmentation where σ_{size} declines with vessel size (see Figure 4). For mixed or regionally focused trades (e.g. Ro-Ro, oil tankers, general cargo), size-aware segmentation is advisable because variability is concentrated in smaller size bins (see Figure 5). For ferries and service vessels,

segmentation by type and size is insufficient; functional segmentation or archetype-based grouping is more appropriate.

Third, the operational indicators derived in this study provide a comprehensive, empirically grounded description of ship operations that can be used as inputs for energy, emissions, and techno-economic modeling. In combination, the metrics capture how vessels are deployed (activity intensity and duty-cycle structure), where and how they operate (routing patterns and spatial exposure), and how this translates into propulsion demand (speed, draught, ME load, and energy demand). Rather than representing isolated parameters, the indicators jointly describe the operational envelope within which ships actually operate over a year. This allows modeling frameworks to parameterize ship operations in a coherent and internally consistent way. The resulting parameter sets therefore reflect real-world operational diversity while remaining tractable for fleet-level applications.

Taken together, the AIS-based variability analysis enables the derivation of operational inputs for energy, emissions, and technology assessment models that balance realism and tractability. It allows empirically grounded representations of ship operations to be retained without requiring vessel-by-vessel simulation, thereby reducing modeling complexity while preserving relevance for fleet-level decision-making.

From a policy and fleet planning perspective, operational variability is informative for where to start with decarbonization. Segments with high representativeness are natural early adopters for alternative fuels and standardized operational measures: predictable travel ranges, stable propulsion and energy demands, and repeatable schedules de-risk fuel logistics and infrastructure utilization (DNV 2025b). Conversely, high-variability segments require flexible energy and infrastructure concepts, such as modular bunkering capacities, hybrid propulsion systems, or dynamic scheduling that can cope with stochastic deployment patterns (Siemens Energy 2022). This asymmetry should also shape the interpretation of regulatory metrics: dispersion in operational profiles implies dispersion in compliance trajectories, even among vessels with similar technical characteristics. Three cross-cutting themes further contextualize these findings.

The North and Baltic Seas context combines dense traffic, short-to-medium routes, and strong port networks (Proximare 2014). The basic hierarchy – uniform liner cargo versus heterogeneous passenger/service – is therefore expected to persist in other regions, although absolute magnitudes of operational variability may shift with weather exposure, voyage lengths, and port topology.

Our sensitivity checks (alternative metric weights and vessel-count weighting) show that the principal findings are robust, yet several methodological choices remain consequential for specific segments: rule-based mode assignment, the 20 KN cap, and the 500 NM routing threshold. These heuristics are defensible but warrant confirmation through data-driven classification in future work.

To bridge from statistics to modeling, four generic archetypes appear practical: (i) highly standardized liner long-haul (stable routing, low dispersion across all metrics); (ii) regional feeder (moderate routing variability, higher draught variability); (iii) tact-scheduled ferry (tight port cycles, high routing and energy intensity dispersion); and (iv) mission-based service (episodic deployment, extreme variation in routing and energy use). Assigning vessels to archetypes within each segment can capture heterogeneity with minimal complexity.

4.2. Limitations

While the North and Baltic Seas provide dense AIS coverage and a wide range of operational patterns, the regional focus of this study constitutes a limitation with respect to the transferability of absolute operational variability values. Shipping activity in these seas is characterized by comparatively short-to-medium voyage lengths, high port-call frequency, and strong network regularity, such that absolute levels of speed, ME load, energy demand, and time allocation may differ from those observed in oceanic trades or less congested regions. Consequently, the results should not be interpreted as globally applicable numerical benchmarks, but as regionally grounded evidence on relative operational variability and representativeness within ship-type and size segments.

This limitation is supplemented by the temporal and fleet-related scope of the analysis. Restricting the dataset to a single year limits the ability to capture longer-term structural changes in routing, utilization, or operational behavior driven by market cycles or regulatory shifts. In addition, the requirement that vessels exhibit at least 30 days of AIS activity within the study area may exclude ships with only episodic regional presence, such as long-haul container services or tankers calling infrequently. While this selection ensures statistical robustness and avoids conflating fundamentally different operational regimes, it also implies that interregional trading patterns and transient port calls are underrepresented. As a result, the derived variability metrics

primarily reflect vessels with sustained regional operations and should be interpreted accordingly.

Like most AIS-based studies, the analysis is subject to inherent data-quality limitations, including irregular updating of static vessel information, positional noise, and inconsistencies in reported draught and speed values. The applied pre-processing steps – including error filtering, conservative speed capping, and trajectory reconstruction with speed and voyage-level draught imputation – mitigate the impact of such artefacts but can not fully eliminate them. Consequently, the derived variability metrics should be interpreted as empirically robust characterizations of operational dispersion rather than as exact physical descriptions of individual vessel behavior.

A specific methodological implication concerns the uniform upper speed cap of 20 KN. This threshold was applied to improve numerical stability and comparability across ship segments, but it may truncate physically realistic operating speeds for passenger-oriented vessels. An inspection of the AIS data shows that speeds above 20 KN occur predominantly in ferry-related segments – most notably Ro-Pax ferries (≈24% of records), passenger ferries (≈10%), and Ro-Ro vessels (≈7%) – while for all other ship types such values account for less than 5% of observations. Given the limited contribution of speed-related metrics to overall operational variability (Section 3.1), this treatment has only a limited influence on the main results. For ship types with systematically higher operating speeds, however, ship-type-specific speed caps would provide a more accurate representation of high-speed operation and represent a natural refinement for future work.

Beyond the speed cap discussed above, additional heuristic thresholds applied throughout the analysis – including the minimum activity-duration requirement, long-voyage cut-off, and distance-to-coast criteria used to define open-sea operation – serve as pragmatic anchors rather than universal definitions. Sensitivity checks indicate that reasonable adjustments to these thresholds do not alter the principal rank ordering of ship segments, but they may affect results for high-speed or mixed-service fleets.

More generally, the rule-based operational mode classification applied in this study prioritizes transparency and reproducibility, but may miss latent sub-patterns, such as nuanced harbor operations or context-specific maneuvering behavior, that could be resolved using supervised or hybrid classification approaches.

Despite these limitations, the three core insights are robust across specifications. First, function dominates: the divide between standardized liner services and demand-driven passenger and service activity is clear and persistent. Second, size stabilizes industrial cargo segments: as vessels scale up, networks and schedules tighten, and variability typically declines. Third, engine and energy metrics dominate variability: models that retain speed distributions but ignore engine load and energy intensity dispersion will likely misrepresent operational diversity.

4.3. Future work

Looking ahead, two complementary development tracks emerge. For research, expand from regional, single-year, rule-based diagnostics to global, multi-year, data-driven segmentation that uncovers operational archetypes and links them to performance metrics (e.g. emissions, compliance). Extending the analysis across multiple sea areas and years would allow testing the stability of observed variability patterns under different market conditions, regulatory regimes, and environmental exposures, and would help distinguish structurally robust patterns from region-specific effects.

For applied modeling, develop segment-specific assumption sets: (i) standardized profiles for high-representativeness segments; (ii) small archetype libraries with probabilistic sampling for mixed segments; and (iii) scenario-based or agent-based treatments for highly variable fleets. Such approaches could incorporate uncertainty ranges derived from observed operational dispersion, rather than relying on single deterministic parameter sets.

Several of the limitations identified in this study also point directly toward future refinements. Uniform heuristic thresholds applied here for transparency and comparability (e.g. speed cap, minimum activity duration) could be replaced or complemented by ship-type- or size-specific thresholds, or by quantile-based trimming strategies that retain realistic high-speed behavior while filtering extreme outliers. This may be particularly relevant for passenger and ferry segments with fundamentally different speed distributions than industrial cargo vessels.

In both tracks, the twelve-metric framework provides a common language to ensure that operational variability becomes an integral, rather than incidental, component of decarbonization assessment. By systematically linking observed operational diversity to modeling assumptions, future work can further improve the credibility of fleet-level energy, emissions, technology uptake, and compliance analyses while preserving transparency and interpretability.

5. Conclusion

This study quantifies how operational variability differs across ship types and size classes in the North and Baltic

Seas, providing a comparable, AIS-based framework that integrates twelve standardized indicators into composite variability scores (σ_{size}, σ_{type}). The analysis demonstrates a clear structural divide: cargo liner segments embedded in fixed networks – especially container, vehicle, and bulk carriers – exhibit low variability, while passenger and service segments show highly dispersed, mission-driven behavior. Within industrial cargo, vessel size often has a stabilizing effect, with σ_{size} typically declining as ships scale up. Across segments, variability is driven primarily by propulsion demand and energy intensity, followed by routing and loading dynamics, whereas speed alone contributes comparatively little – implying limited value in refining speed assumptions without jointly calibrating engine load and energy intensity parameters.

These insights translate directly into practice. For modeling, standardized duty cycles and stable parameter sets are defensible for high-representativeness cargo segments; mixed trades benefit from size-aware treatments; and highly variable fleets call for archetype- or scenario-based representations that sample operational heterogeneity explicitly. The twelve-metric framework offers a practical calibration kit, mapping duty cycle shares, routing fractions, and engine/energy profiles into fleet and policy models. For policy and industry, early adoption of alternative fuels and fixed logistics should concentrate on low variability segments, while ferries and service vessels require flexible energy solutions and adaptable infrastructure planning.

Limitations include the single-year and regional focus, and the use of rule-based mode assignment and pragmatic thresholds; nonetheless, robustness checks against metric weighting and vessel-count imbalances support the stability of the main findings. Future work should extend the analysis across years and regions, develop data-driven operational archetypes, and link variability measures to compliance and retrofit pathways. By embedding observed variability – not idealized behavior – into assessments, the proposed framework enables more credible decarbonization strategies that align with how ships actually operate.

Author contributions

CRediT: **Joost Hobbie:** Conceptualization, Formal analysis, Methodology, Software, Visualization, Writing – original draft; **Ishan Sontakke:** Validation, Writing – review & editing; **Thorben Schwedt:** Data curation, Software; **Martin Bergström:** Conceptualization, Supervision, Writing – review & editing; **Sören Ehlers:** Supervision.

Disclosure statement

No potential conflict of interest was reported by the author(s).

Notes on contributors

Joost Hobbie is a Research Scientist at the German Aerospace Centre (DLR), Institute of Maritime Technologies and Propulsion Systems, since June 2024. He holds a Master's degree in Operation and Management of Maritime Systems from the University of Applied Sciences Wismar (Germany) and has a professional background in maritime economics and logistics. His work focuses on maritime transport systems and fleet development, with an emphasis on techno-economic assessment, modeling of ship operations, and life-cycle cost and emission analyses.

Ishan Sontakke holds a Master's degree in Operations and Management of Maritime Systems from the University of Applied Sciences Wismar (Germany). His work focuses on techno-economic assessment, fleet simulation, and optimization of alternative fuels, retrofit strategies, and regulatory compliance. Since March 2024, He has been working as a researcher at the German Aerospace Centre (DLR) - Institute of Maritime Technologies and Propulsion Systems. His research interests include decision-support methods, investment decision-making, and practical transition planning for low-emission shipping under technical, economic, and policy uncertainty.

Thorben Schwedt is a researcher at the German Aerospace Center (DLR), Institute of Maritime Technologies and Propulsion Systems. He holds a Master's degree in Physics from the University of Göttingen (Germany). His work focuses on route and speed optimization, with an emphasis on wind-assisted propulsion. He also conducts AIS-based analyses of vessel operations, power demand, and emissions, as well as onboard measurement campaigns.

Dr. Martin Bergström has a master's degree in Naval Architecture from Aalto University (Finland) and a doctoral degree in Maritime Technology from the Norwegian University of Science and Technology. In his doctoral project, he developed a simulation-based method for the conceptual design of safe and cost-efficient Arctic maritime transport systems. Following his PhD graduation in 2017, he conducted postdoctoral research at Aalto University on a range of topics concerning the design and operation of ships, including modelling and simulation of maritime operations, risk and efficiency assessments, and regulatory development. Since May 2022, he has been working at the German Aerospace Centre (DLR) - Institute of Maritime Technologies and Propulsion Systems on issues related to the integration of innovative technologies in ships and maritime transport systems.

Prof. D.Sc. (Tech.) Sören Ehlers studied mechanical engineering at the University of Rostock (Germany), specializing in shipbuilding and marine technology. He received his doctorate from the Helsinki University of Technology (Finland) in 2009 and worked there as a post-doctoral researcher. He also co-founded an engineering office that is still in operation today. In 2011, he became a professor at NTNU in Trondheim (Norway) and focused on Arctic Sea transportation and ship design under ice loads. Since 2014, he held the position of professor of design and strength of ships and offshore structures at Hamburg University of Technology (Germany) and lead the corresponding institute until his leave of absence to work for the German Aerospace Center (DLR) from 2022 as a director of the Institute of Maritime Technologies and Propulsion Systems.

Data availability statement

Data not available due to commercial restrictions.

ORCID

Joost Hobbie http://orcid.org/0009-0008-2050-5010
Ishan Sontakke http://orcid.org/0009-0001-6581-5038
Thorben Schwedt http://orcid.org/0000-0002-2127-0494
Martin Bergström http://orcid.org/0000-0001-7758-3038
Sören Ehlers http://orcid.org/0000-0001-5698-9354

References

ABL Group. 2021. NORTH AND BALTIC SEA. Navigation Shipping Study. Expert's study on shipping traffic flows in the North and Baltic Seas and options to enhance the safety of shipping in the future. Work Package 1 – Traffic Study Report; [accessed 2026 Jan 6]. https://www.bsh.de/EN/TOPICS/Offshore/Maritime_spatial_planning/Maritime_Spatial_Plan_2021/_Anlagen/Downloads/Schifffahrtsgutachten/Report_Traffic_Analysis.pdf?__blob=publicationFile&v=2

Aulinger A et al. 2016. The impact of shipping emissions on air pollution in the greater North Sea region – Part 1: current emissions and concentrations. Atmos Chem Phys. 16(2):739–758. https://doi.org/10.5194/acp-16-739-2016

Bergström M et al. 2023. A simulation-based approach for evaluating merchant fleet decarbonization strategies. In: Proceedings of the 42nd International Conference on Ocean, Offshore and Arctic Engineering; June 11-16; Melbourne, Australia. American Society of Mechanical Engineers. https://doi.org/10.1115/OMAE2023-102401

Chen X, Liu Y, Achuthan K, Zhang X. 2020. A ship movement classification based on Automatic Identification System (AIS) data using Convolutional Neural Network. Ocean Eng. 218:108182. https://doi.org/10.1016/j.oceaneng.2020.108182

Clarksons Research. 2025. World Fleet Register; [accessed 2026 Jan 6]. https://www.clarksons.net/wfr

Comer B, Stolz D, Mao X, Osipova L. 2022. Decarbonizing bulk carriers with hydrogen fuel cells and wind-assisted propulsion: a modeled case study analysis; [accessed 2026 Jan 6]. https://theicct.org/sites/default/files/publications/Hydrogen-and-propulsion-ships-jan22.pdf

Cullinane K, Khanna M.. 2000. Economies of scale in large containerships: optimal size and geographical implications. J Transp Geogr. 8(3):181–195. https://doi.org/10.1016/S0966-6923(00)00010-73

Derrett D. 2005. Ship stability for masters and mates. 5th ed. Butterworth-Heinemann.

DNV. 2022. Nordic roadmap: future fuels for shipping; [accessed 2026 Jan 6]. https://futurefuelsnordic.com/wp-content/uploads/2022/11/AIS-Analysis-of-Nordic-Ship-Traffic.pdf#:~:text=,for%20most%20of%20the%20traffic

DNV. 2025a. Energy-efficiency measures and technologies; [accessed 2026 Jan 6]. https://www.dnv.com/maritime/publications/energy-efficiency-report-download/

DNV. 2025b. Maritime Forecast to 2050; [accessed 2026 Jan 6]. https://www.dnv.com/maritime/maritime-forecast/

Elmallah M et al. 2025. Decarbonization potential of alternative fuels in container shipping: a case study of the EVER ALOT Vessel. Environments. 12(9):306. https://doi.org/10.3390/environments12090306

EMSA. 2021. IMPACT OF COVID-19 ON THE MARITIME SECTOR IN THE EU; [accessed 2026 Jan 6]. https://south.euneighbours.eu/wp-content/uploads/2022/07/EMSA_Impact_of_the_COVID_19_EN-3.pdf

EU. 2023. Regulation (EU) 2023/1805 of the European Parliament and of the Council of 13 September 2023 on the use of renewable and low-carbon fuels in maritime transport, and amending Directive 2009/16/EC.

EU. 2024. Directive 2003/87/EC of the European Parliament and of the Council of 13 October 2003 establishing a system for greenhouse gas emission allowance trading within the Union and amending Council Directive 96/61/EC.

Fan A et al. 2024. Data-driven ship typical operational conditions: a benchmark tool for assessing ship emissions. J Cleaner Prod. 483:144252. https://doi.org/10.1016/j.jclepro.2024.144252

Flanders Marine Institute. 2018. IHO Sea Areas, version 3; [accessed 2026 Jan 6]. https://www.marineregions.org/downloads.php

Godet A, Panagakos G, Barfod MB, Lindstad E. 2024. Operational cycles for maritime transportation: consolidated methodology and assessments. Transp Res D-Transp Environ. 132:104238. https://doi.org/10.1016/j.trd.2024.104238

Gucma L, Raczkowska J.. 2018. An analysis of basic parameters of Ro-Pax Ferries in the Baltic Sea as guidelines for its preliminary design. Pol Marit Res. 25(3):44–53. https://doi.org/10.2478/pomr-2018-0095

Harati-Mokhtari A, Wall A, Brooks P, Wang J. 2007. Automatic Identification System (AIS): data reliability and human error implications. J. Navigation. 60:373–389. https://doi.org/10.1017/S0373463307004298

HELCOM. 2009. Ensuring safe shipping in the Baltic; [accessed 2026 Jan 6]. https://helcom.fi/wp-content/uploads/2019/10/Ensuring-safe-shipping-in-the-Baltic.pdf

IALA. 2016. IALA Guideline: G1082 an overview of AIS; [accessed 2026 Jan 6]. https://www.iala.int/product/g1082/

IHO. 1953. Limits of oceans and seas: special publication No. 23. Monégasque.

IMO. 1914. International convention for the safety of life at sea.

IMO. 2015. Third IMO Greenhouse Gas Study; [accessed 2026 Jan 6]. https://wwwcdn.imo.org/localresources/en/OurWork/Environment/Documents/Third%20Greenhouse%20Gas%20Study/GHG3%20Executive%20Summary%20and%20Report.pdf

IMO. 2021. Fourth IMO Greenhouse Gas Study; [accessed 2026 Jan 6]. https://wwwcdn.imo.org/localresources/en/OurWork/Environment/Documents/Fourth%20IMO%20GHG%20Study%202020%20-%20Full%20report%20and%20annexes.pdf

IMO. 2023. Resolution MEPC.377(80) (adopted on 7 July 2023) 2023 IMO strategy on reduction of GHG emissions from ships.

Jafarzadeh S, Schjølberg I. 2018. Operational profiles of ships in Norwegian waters: an activity-based approach to assess the benefits of hybrid and electric propulsion. Transp Res D-Transp Environ. 65:500–523. https://doi.org/10.1016/j.trd.2018.09.021

Jalkanen J, Johansson L, Kukkonen J.. 2016. A comprehensive inventory of ship traffic exhaust emissions in the European

sea areas in 2011. Atmos Chem Phys. 16(1):71–84. https://doi.org/10.5194/acp-16-71-2016

Kanchiralla FM et al. 2023. How do variations in ship operation impact the techno-economic feasibility and environmental performance of fossil-free fuels? A life cycle study. Appl Energy. 350:121773. https://doi.org/10.1016/j.apenergy.2023.121773

Kim J, Choi J.. 2023. A study on analysis of green house gaseous emitted from ships through operation information. J Int Marit Saf Environ Aff Shipp. 7(2–3). https://doi.org/10.1080/25725084.2023.2234163

Kontopoulos I, Varlamis I, Tserpes K.. 2021. A distributed framework for extracting maritime traffic patterns. Int J Geogr Inf Sci. 35(4):767–792. https://doi.org/10.1080/13658816.2020.1792914

Ksciuk J, Kuhlemann S, Tierney K, Koberstein A.. 2023. Uncertainty in maritime ship routing and scheduling: a literature review. Eur J Oper Res. 308(2):499–524. https://doi.org/10.1016/j.ejor.2022.08.006

Li G et al. 2024. An approach for traffic pattern recognition integration of ship AIS data and port geospatial features. Geo-spat Inf Sci. 27(6):2048–2075. https://doi.org/10.1080/10095020.2024.2308715

Martincic T, Stepec D, Costa JP, Cagran K, Chaldeakis A. 2020. Vessel and port efficiency metrics through validated AIS data. In: Proceedings of the Global Oceans 2020: Singapore – U.S. Gulf Coast Conference; Oct 5-30; Biloxi, USA. IEEE. https://doi.org/10.1109/IEEECONF38699.2020.9389112

Natural Earth. 2009a. 1.10m cultural vectors. Ports. Version 5.0.0; [accessed 2026 Jan 6]. https://www.naturalearthdata.com/downloads/10m-cultural-vectors/ports/

Natural Earth. 2009b. 1:10m physical vectors. Coastline. Version 4.1.0; [accessed 2026 Jan 6]. https://www.naturalearthdata.com/downloads/10m-physical-vectors/10m-coastline/

Oh M et al. 2021. Operational analysis of container ships by using maritime big data. JMSE. 9(4):438. https://doi.org/10.3390/jmse9040438

Olmer N, Comer B, Biswajoy R, Xiaoli M, Rutherford D. 2017. Greenhouse gas emissions from global shipping, 2013-2015; [accessed 2026 Jan 6]. https://theicct.org/wp-content/uploads/2021/06/Global-shipping-GHG-emissions-2013-2015_ICCT-Report_17102017_vF.pdf

Park J, Choi M.. 2022. A K-means clustering algorithm to determine representative operational profiles of a ship using AIS data. JMSE. 10(9):1245. https://doi.org/10.3390/jmse10091245

Proximare. 2014. North Sea – Baltic core network corridor study; [accessed 2026 Jan 6]. https://transport.ec.europa.eu/system/files/2017-06/north_sea-baltic_study_0.pdf

Ramboll. 2022. Kraftstoffanalyse In Der Schifffahrt Nach Segmenten; [accessed 2026 Jan 6]. https://dmz-maritim.de/wp-content/uploads/2022/06/20220601-Kraftstoffanalyse-in-der-Schifffahrt-nach-Segmenten-final.pdf

Rodrigue J. 2024. The geography of transport systems. Routledge.

Schwarzkopf DA et al. 2021. A ship emission modeling system with scenario capabilities. Atmospheric Environment: X. 12:100132. https://doi.org/10.1016/j.aeaoa.2021.100132

Siemens Energy. 2022. How to cut Europe's ferry emissions in half; [accessed 2026 Jan 6]. https://www.siemens-energy.com/us/en/home/stories/the-electrification-of-europes-ferry-fleet.html

Stopford M. 2009. Maritime economics. 3rd ed. Routledge.

Sys C, Blauwens G, Omey E, van de Voorde E, Witlox F.. 2008. In search of the link between ship size and operations. Transp Plan Technol. 31(4):435–463. https://doi.org/10.1080/03081060802335109

Trivyza NL, Rentizelas A, Theotokatos G. 2016. The influence of ship operational profile in the sustainability of ship energy systems. In: Proceedings of the International Conference of Maritime Safety and Operations; Oct 13-14; Glasgow, UK. University of Strathclyde.

Tsiotas D, Ducruet C. 2021. Measuring the effect of distance on the network topology of the Global Container Shipping Network. Sci Rep. 11:21250. https://doi.org/10.1038/s41598-021-00387-3

UN. 1984. United Nations Convention on the Law of the Sea.

UNCTAD. 2021. Review of Maritime Transport 2021; [accessed 2026 Jan 6]. https://unctad.org/system/files/official-document/rmt2021_en_0.pdf

Yi W et al. 2025. The high-resolution global shipping emission inventory by the Shipping Emission Inventory Model (SEIM). Earth Syst Sci Data. 17(1):277–292. https://doi.org/10.5194/essd-17-277-2025

Zhao L, Shi G, Yang J.. 2018. Ship trajectories pre-processing based on AIS data. J Navigation. 71(5):1210–1230. https://doi.org/10.1017/S0373463318000188

Zhou Y, Daamen W, Vellinga T, Hoogendoorn SP. 2019. Ship classification based on ship behavior clustering from AIS data. Ocean Eng. 175:176–187. https://doi.org/10.1016/j.oceaneng.2019.02.005